MIXED CONVECTIVE AND RADIATIVE HEAT TRANSFER IN A HORIZONTAL CONCENTRIC AND ECCENTRIC CYLINDRICAL ANNULI

Ass. Prof. Manal Hadi Al-Hafidh
Mech. Engr. Dept.
College of Engineering
University of Baghdad

Lina S. Safwat
Mechanical Engineer
Ishtar_l21@yahoo.com

ABSTRACT

A numerical investigation has been performed to study the effect of eccentricity on unsteady state, laminar aiding mixed convection in a horizontal concentric and eccentric cylindrical annulus. The outer cylinder was kept at a constant temperature while the inner cylinder was heated with constant heat flux. The study involved numerical solution of transient momentum (Navier-Stokes) and energy equation using finite difference method (FDM), where the body fitted coordinate system (BFC) was used to generate the grid mesh for computational plane. The governing equations were transformed to the vorticity-stream function formula as for momentum equations and to the temperature and stream function for energy equation.

A computer program (Fortran 90) was built to calculate the bulk Nusselt number (Nu_b) after reaching steady state condition for fluid Prandtl number fixed at 0.7 (air) with radius ratio ($\bar{R}$=2.6), Rayleigh number (Ra=200), Reynolds number (Re=50) for both concentric and eccentric cylindrical annulus with different eccentricity ratios (ε=0, 0.25, 0.50, 0.75) and angular positions (φ_o=0°, 45°, 90°, 135°, 180°).

The results show a reasonable representation to the relation between Nusselt number and (ε, φ_o). Generally, $\boldsymbol{Nu_b}$ decreased with the increase in (ε and φ_o). Also, results show that the best thermal performance for the inner cylinder was at the angular position (φ_o=0°) for eccentricity ratio (ε=0.25), while the maximum reduction in the rate of heat transfer for the inner cylinder was at the angular position (φ_o=180°) for eccentricity ratio (ε=0.75).

Comparison of the result with the previous work shows a good agreement.

الخلاصة

تم إجراء بحث عددي لدراسة تأثير اللامركزية لجريان مختلط مساعد غير مستقر يقع بين اسطوانتين أفقيتين متحدة وغير متحدة المركز، تم حفظ الاسطوانة الخارجية بدرجة حرارة ثابتة بينما سخنت الاسطوانة الداخلية بفيض حراري ثابت . بينت الدراسة النظرية حل عددي لمعادلات الزخم والطاقة لمسألة البحـث باسـتخدام طريقة الفروقات المحددة وتم استخدام نظام الإحداثيات المطابقة للجسم (BFC) في توليد شـبكة العقـد بعـد تحويل هذه المعادلات إلى صيغة دالة الانسياب-الدوامية .

تم بناء برنامج (فورتران 90) لحساب رقم نسلت (Nu) بعد الوصول إلى حالة الاستقرار لقيمة رقم برانتل ثابتة 0.7 (هواء) ولنسبة نصف قطر ($\bar{R}$=2.6) ولخواص جريان ممثلة برقم رينولد (Re=50) ورقم رالـي (Ra=200) لحالتي الاسطوانتين المتحدة وغير متحدة المركز لنسب لامركزية (ε=0, 0.25, 0.50, 0.75) ولموقع زاوي للاسطوانة الداخلية ضمن التجويف (φ_o= 0°, 45°, 90°, 135°, 180°)

أعطت النتائج تمثيلاً معقولا لمعدل رقم نسلت بواسطة رسم مخططات تمثل تأثيركل من (φ_o, ε) على قيمة *Nu* . وبصورة عامة وجد إن رقم نسلت يقل مع زيادة (φ_o , ε). وبينت النتائج أيضا ان أفضل أداء حراري للاسطوانة الداخلية كان في الموقع الزاوي (φ_o=0°) ولنسبة لامركزية (ε=0.25) بينما كان أعظم انخفـاض في معدل انتقال الحرارة للاسطوانة الداخلية في الموقع الزاوي (φ_o=180°) ولنسبة لامركزية (ε=0.75). تم إجراء مقارنة مع البحوث السابقة وكانت جيدة.

KEY WORDS: Flow and Heat Transfer, Laminar, Mixed Convection, Concentric and Eccentric, Horizontal Annulus.

INTRODUCTION:

The process of heating and cooling of the flowing fluids inside channels was considered as one of the important subjects in heat transfer problems. Many researchers studied the heat transfer and fluid flow through the channels with different cross section areas to attain the best performance of the heat exchanger.

Mixed convection heat transfer in horizontal ducts of concentric and eccentric cylindrical annular form has received increased attention due to the interesting feature of specific heat transfer phenomenon and fundamental importance in practical applications.

An experimental and theoretical study has been conducted by [**Akeel Al−Sudani, 2005**] on mixed convection heat transfer of the flow through an inclined concentric annulus with uniformly heated inner cylinder and adiabatic outer cylinder with both fixed and rotating inner cylinder, little researches dealt with mixed convection in an eccentric annulus. [**William, 1963**], presented a solution for the temperature distribution in a fluid flowing in an eccentric annulus formed with circular cylinders under the assumption of slug flow. [**Shu and Wu, 2001**], presented an efficient numerical approach of using domain-free discretization method to solve partial differential equations on a doubly connected domain concentric and eccentric annulus. The consideration in the present study is given to laminar unsteady state mixed convection with radiation in concentric and eccentric horizontal annuls with the outer cylinder maintained isothermal while the inner cylinder was subjected to a uniform constant heat flux. **Fig. (1)** shows the annulus geometry and coordinate system of the problem under consideration

Important applications for mixed convection in an annulus may be summarized as follows: Double pipe heat exchangers, heating processes in nuclear reactors, the cooling of electrical equipments, the design of certain types of solar energy collectors and heating of process fluids [**Yasin et.al 2006**].

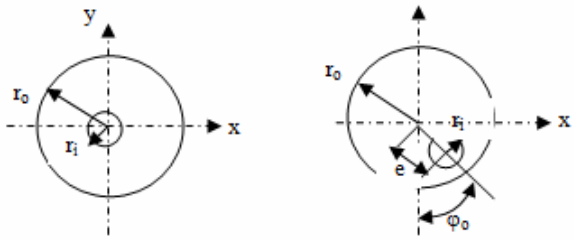

Figure (1) Schematic of the Present Study

GOVERNING EQUATIONS:

Unsteady steady state, quasi three-dimensional, incompressible, fully developed laminar aiding air flow was investigated.

Accordingly the governing, continuity, momentum and energy conservation equations were as follows:-

Continuity equation:

$$\frac{\partial u}{\partial x}+\frac{\partial v}{\partial y}=0 \qquad (1)$$

Momentum Equations:

$$\frac{\partial u}{\partial t}+u\frac{\partial u}{\partial x}+v\frac{\partial u}{\partial y}=-\frac{1}{\rho}\frac{dp}{dx}+\nu\left[\frac{\partial^2 u}{\partial x^2}+\frac{\partial^2 u}{\partial y^2}\right] \qquad (2)$$

$$\frac{\partial v}{\partial t}+u\frac{\partial v}{\partial x}+v\frac{\partial v}{\partial y}=-\frac{1}{\rho}\frac{dp}{dy}+\nu\left[\frac{\partial^2 v}{\partial x^2}+\frac{\partial^2 v}{\partial y^2}\right]+g\beta(T-T_w) \qquad (3)$$

$$\frac{\partial w}{\partial t}+u\frac{\partial w}{\partial x}+v\frac{\partial w}{\partial y}=-\frac{1}{\rho}\frac{dp}{dz}+\nu\left[\frac{\partial^2 w}{\partial x^2}+\frac{\partial^2 w}{\partial y^2}\right] \qquad (4)$$

Energy Equation:

$$\frac{\partial T}{\partial t}+u\frac{\partial T}{\partial x}+v\frac{\partial T}{\partial y}+w\frac{\partial T}{\partial z}=\alpha\left[\frac{\partial^2 T}{\partial x^2}+\frac{\partial^2 T}{\partial y^2}\right]+\frac{4\sigma k_r e T_w^4}{\rho c_p}(T_w-T) \quad (5)$$

The dimensionless parameters:

$\tau=\frac{\nu t}{De^2}$, $De = 2(r_o - r_i)$,

$X=\frac{x}{De}$, $Y=\frac{y}{De}$,

$Z=\frac{z}{De}$, $\varepsilon=\frac{e}{De}$, $U=\frac{uDe}{\nu}$,

$V=\frac{vDe}{\nu}$,

$W=\frac{wDe}{\nu}$, $\theta=\frac{(T_w-T)}{PrCDe}$,

$P=\frac{PDe^2}{\rho\nu^2}$, $Pr=\frac{\nu}{\alpha}$, $Ra=\frac{g\beta CDe^4}{\nu\alpha}$,

$C=\frac{\partial T}{\partial z}$, $A=-\frac{4\rho\nu^2\hat{R}e}{De^3}$,

$\hat{R}=\frac{r_o}{r_i}$, $N=\frac{4\sigma e T_w^3}{k k_r}$, $\hat{t}=k_r De$

By using these dimensionless forms, the above equations can be written as follows.

$$\frac{\partial U}{\partial X}+\frac{\partial V}{\partial Y}=0 \quad (6)$$

$$\frac{\partial U}{\partial \tau}+U\frac{\partial U}{\partial X}+V\frac{\partial U}{\partial Y}=-\frac{dP}{dX}+\left[\frac{\partial^2 U}{\partial X^2}+\frac{\partial^2 U}{\partial Y^2}\right] \quad (7)$$

$$\frac{\partial V}{\partial \tau}+U\frac{\partial V}{\partial X}+V\frac{\partial V}{\partial Y}=-\frac{dP}{dY}+\left[\frac{\partial^2 V}{\partial X^2}+\frac{\partial^2 V}{\partial Y^2}\right]-Ra\,\theta \quad (8)$$

$$\frac{\partial W}{\partial \tau}+U\frac{\partial W}{\partial X}+V\frac{\partial W}{\partial Y}=\left[\frac{\partial^2 W}{\partial X^2}+\frac{\partial^2 W}{\partial Y^2}\right]+4Re \quad (9)$$

$$\frac{\partial \theta}{\partial \tau}+U\frac{\partial \theta}{\partial X}+V\frac{\partial \theta}{\partial Y}=\frac{1}{Pr}\left[\frac{\partial^2 \theta}{\partial X^2}+\frac{\partial^2 \theta}{\partial Y^2}\right]+\frac{W}{Pr}+\frac{N\hat{t}^2\theta}{Pr} \quad (10)$$

The governing equations in dimensionless form above were written in terms of dependant variables (U, V, W, P, θ). The pressure term in the momentum equations will be eliminated in the resulting vorticity equation as can be shown below:

$$\frac{\partial \Omega}{\partial \tau}+U\frac{\partial \Omega}{\partial X}+V\frac{\partial \Omega}{\partial Y}=\left[\frac{\partial^2 \Omega}{\partial X^2}+\frac{\partial^2 \Omega}{\partial Y^2}\right]-Ra\frac{\partial \theta}{\partial X} \quad (11)$$

For this flow field, the only non-zero component of the vorticity is:

$$\Omega=\frac{\partial V}{\partial X}-\frac{\partial U}{\partial Y} \quad (12)$$

Also by making use of the vorticity definition of equation (12) and the definition of stream function (Ψ), which satisfy continuity equation, the horizontal and vertical velocities can be written as follows respectively:-

$$U=\frac{\partial \Psi}{\partial Y} \quad (13)$$

$$V=-\frac{\partial \Psi}{\partial X} \quad (14)$$

By substituting the velocity components of equations (13) and (14) in the vorticity definition equation (12) , stream function equation resulted as :-

$$-\Omega=\left[\frac{\partial^2 \Psi}{\partial X^2}+\frac{\partial^2 \Psi}{\partial Y^2}\right] \quad (15)$$

Boundary Nodes:

The positions of the inner and outer cylinders can be represented by the eccentricity (ε) and the angular position (φ_o), where ($0^o \le \varphi_o \le 360°$).

For an eccentric annulus, the origin was put at the center of the inner cylinder. So, $r_i(\varphi)$ was a constant, but $r_o(\varphi)$ was a function of **φ.** If the radius ratio is defined as $\tilde{R} = \frac{r_o}{r_i}$, then the non-dimensional radii of the inner and outer cylinders are $R_i=1/(\tilde{R}-1)$ and $R_o=\tilde{R}/(\tilde{R}-1)$. Therefore, $r_i(\varphi)$ and $r_o(\varphi)$ are given by [**Shu and Wu 2001**] :-

$$r_i(\varphi) = R_i = \frac{1}{(\tilde{R}-1)} \tag{16}$$

$$r_o(\varphi) = -\varepsilon\cos(\varphi-\varphi_o) + [R_o^2 - \varepsilon^2\sin^2(\varphi-\varphi_o)]^{1/2} \tag{17}$$

Initial Conditions:

Initial conditions may be chosen as zero:

At $\tau = 0$,

U = V = W = Ω = Ψ = 0 [No slip condition]

The boundary conditions which defined by [**Kotake and Hattori 1985**] and [**Kaviany 1986**], making use that the boundary conditions for a motionless rigid surface which required that both horizontal and vertical velocities components (U and V) to be vanished at surface.

This expressed in terms of stream function as follows:-

- Inner cylinder surface :

$$U = V = W = \Psi = 0 \quad , \quad \Omega = -\left.\frac{\partial^2\Psi}{\partial r^2}\right|_w \quad , \quad \theta_i = 0 \tag{18}$$

- Outer cylinder surface :

$$U = V = W = \Psi = 0 \quad , \quad \Omega = -\left.\frac{\partial^2\Psi}{\partial r^2}\right|_w \quad , \quad \frac{\partial\theta_o}{\partial n} = 0 \tag{19}$$

TRANSFORMATION OF GOVERNING EQUATIONS:-

Governing equations can be transformed from the Cartesian coordinates (X,Y) to generalized coordinates (ζ, η) as shown below:

1- Vorticity-Transport Equation:-

$$\frac{\partial\Omega}{\partial\tau} + \frac{(\Psi_\eta\Omega_\zeta - \Psi_\zeta\Omega_\eta)}{J} = \frac{(\varrho\Omega_\zeta + \varpi\Omega_\eta + \alpha\Omega_{\zeta\zeta} - 2\beta\Omega_{\zeta\eta} + \gamma\Omega_{\eta\eta})}{J^2} - Ra\frac{(\theta_\zeta Y_\eta - \theta_\eta Y_\zeta)}{J} \tag{20}$$

2- Axial Momentum Equation:-

$$\frac{\partial W}{\partial\tau} + \frac{(\Psi_\eta W_\zeta - \Psi_\zeta W_\eta)}{J} = \frac{(\varrho W_\zeta + \varpi W_\eta + \alpha W_{\zeta\zeta} - 2\beta W_{\zeta\eta} + \gamma W_{\eta\eta})}{J^2} + 4Re \tag{21}$$

3- Energy equation :-

$$\frac{\partial\theta}{\partial\tau} + \frac{(\Psi_\eta\theta_\zeta - \Psi_\zeta\theta_\eta)}{J} = \frac{1}{Pr}\left[\frac{(\varrho\theta_\zeta + \varpi\theta_\eta + \alpha\theta_{\zeta\zeta} - 2\beta\theta_{\zeta\eta} + \gamma\theta_{\eta\eta})}{J^2} + W + Nt^2\theta\right] \tag{22}$$

4- Stream Function Equation:-

$$-\Omega = \frac{(\varrho\Psi_\zeta + \varpi\Psi_\eta + \alpha\Psi_{\zeta\zeta} - 2\beta\Psi_{\zeta\eta} + \gamma\Psi_{\eta\eta})}{J^2} \tag{23}$$

5- Vertical Velocity:-

$$V = \frac{(\Psi_\eta Y_\zeta - \Psi_\zeta Y_\eta)}{J} \tag{24}$$

6- Horizontal Velocity:-

$$U = \frac{(\Psi_\eta X_\zeta - \Psi_\zeta X_\eta)}{J} \tag{25}$$

NUMERICAL SOLUTION:

Explicit finite difference technique was the numerical method used for solving the transient behavior of the fluid flow and heat transfer until the steady state was reached by marching out in time steps ($\Delta\tau$).

1- Discretization of Vorticity Equation:-

$$\Omega^{n+1}_{(i,j)} = A_1\Omega^n_{(i+1,j)} + A_2\Omega^n_{(i-1,j)} + A_3\Omega^n_{(i,j)} + A_4\Omega^n_{(i,j+1)} + A_5\Omega^n_{(i,j-1)} - A_6\left(\Omega^n_{(i+1,j+1)} - \Omega^n_{(i+1,j-1)} - \Omega^n_{(i-1,j+1)} + \Omega^n_{(i-1,j-1)}\right) - A_7 \quad (26)$$

Where:-

$$A_1 = \frac{\varphi_{(i,j)}\Delta\tau}{2J^2_{(i,j)}\Delta\zeta} + \frac{\alpha_{(i,j)}\Delta\tau}{J^2_{(i,j)}\Delta\zeta^2} - \frac{E\Delta\tau}{4\Delta\zeta\Delta\eta J_{(i,j)}} \quad (27\text{-a})$$

$$A_2 = -\frac{\varphi_{(i,j)}\Delta\tau}{2J^2_{(i,j)}\Delta\zeta} + \frac{\alpha_{(i,j)}\Delta\tau}{J^2_{(i,j)}\Delta\zeta^2} + \frac{E\Delta\tau}{4\Delta\zeta\Delta\eta J_{(i,j)}} \quad (27\text{-b})$$

$$A_3 = 1 - \frac{2\alpha_{(i,j)}\Delta\tau}{J^2_{(i,j)}\Delta\zeta^2} - \frac{2\gamma_{(i,j)}\Delta\tau}{J^2_{(i,j)}\Delta\eta^2} \quad (27\text{-c})$$

$$A_4 = \frac{\varpi_{(i,j)}\Delta\tau}{2J^2_{(i,j)}\Delta\eta} + \frac{\gamma_{(i,j)}\Delta\tau}{J^2_{(i,j)}\Delta\eta^2} + \frac{F\Delta\tau}{4\Delta\zeta\Delta\eta J_{(i,j)}} \quad (27\text{-d})$$

$$A_5 = -\frac{\varpi_{(i,j)}\Delta\tau}{2J^2_{(i,j)}\Delta\eta} + \frac{\gamma_{(i,j)}\Delta\tau}{J^2_{(i,j)}\Delta\eta^2} - \frac{F\Delta\tau}{4\Delta\zeta\Delta\eta J_{(i,j)}} \quad (27\text{-e})$$

$$A_6 = \frac{\beta_{(i,j)}\Delta\tau}{2J^2_{(i,j)}\Delta\zeta\Delta\eta} \quad (27\text{-f})$$

$$A_7 = \frac{Ra\Delta\tau}{J_{(i,j)}}\left[\left(\frac{\theta_{(i+1,j)}-\theta_{(i-1,j)}}{2\Delta\zeta} * \frac{Y_{(i,j+1)}-Y_{(i,j-1)}}{2\Delta\eta}\right) - \left(\frac{\theta_{(i,j+1)}-\theta_{(i,j-1)}}{2\Delta\eta} * \frac{Y_{(i+1,j)}-Y_{(i-1,j)}}{2\Delta\zeta}\right)\right] \quad (27\text{-g})$$

2- Discretization of Axial Momentum Equation :-

$$W^{n+1}_{(i,j)} = B_1W^n_{(i+1,j)} + B_2W^n_{(i-1,j)} + B_3W^n_{(i,j)} + B_4W^n_{(i,j+1)} + B_5W^n_{(i,j-1)} - B_6\left(W^n_{(i+1,j+1)} - W^n_{(i+1,j-1)} - W^n_{(i-1,j+1)} + W^n_{(i-1,j-1)}\right) + B_7 \quad (28)$$

Where:-

$$B_1 = \frac{\varphi_{(i,j)}\Delta\tau}{2J^2_{(i,j)}\Delta\zeta} + \frac{\alpha_{(i,j)}\Delta\tau}{J^2_{(i,j)}\Delta\zeta^2} - \frac{E\Delta\tau}{4\Delta\zeta\Delta\eta J_{(i,j)}} \quad (29\text{-a})$$

$$B_2 = -\frac{\varphi_{(i,j)}\Delta\tau}{2J^2_{(i,j)}\Delta\zeta} + \frac{\alpha_{(i,j)}\Delta\tau}{J^2_{(i,j)}\Delta\zeta^2} + \frac{E\Delta\tau}{4\Delta\zeta\Delta\eta J_{(i,j)}} \quad (29\text{-b})$$

$$B_3 = 1 - \frac{2\alpha_{(i,j)}\Delta\tau}{J^2_{(i,j)}\Delta\zeta^2} - \frac{2\gamma_{(i,j)}\Delta\tau}{J^2_{(i,j)}\Delta\eta^2} \quad (29\text{-c})$$

$$B_4 = \frac{\varpi_{(i,j)}\Delta\tau}{2J^2_{(i,j)}\Delta\eta} + \frac{\gamma_{(i,j)}\Delta\tau}{J^2_{(i,j)}\Delta\eta^2} + \frac{F\Delta\tau}{4\Delta\zeta\Delta\eta J_{(i,j)}} \quad (29\text{-d})$$

$$B_5 = -\frac{\varpi_{(i,j)}\Delta\tau}{2J^2_{(i,j)}\Delta\eta} + \frac{\gamma_{(i,j)}\Delta\tau}{J^2_{(i,j)}\Delta\eta^2} - \frac{F\Delta\tau}{4\Delta\zeta\Delta\eta J_{(i,j)}} \quad (29\text{-e})$$

$$B_6 = \frac{\beta_{(i,j)}\Delta\tau}{2J^2_{(i,j)}\Delta\zeta\Delta\eta} \quad (29\text{-f})$$

$$B_7 = \Delta\tau\left(4Re - Ra\theta_{(i,j)}\sin\delta\right) \quad (29\text{-g})$$

3- Discretization of Energy Equation :-

$$\theta^{n+1}_{(i,j)} = C_1\theta^n_{(i+1,j)} + C_2\theta^n_{(i-1,j)} + C_3\theta^n_{(i,j)} + C_4\theta^n_{(i,j+1)} + C_5\theta^n_{(i,j-1)} - C_6\left(\theta^n_{(i+1,j+1)} - \theta^n_{(i+1,j-1)} - \theta^n_{(i-1,j+1)} + \theta^n_{(i-1,j-1)}\right) + C_7 \quad (30)$$

Where:-

$$C_1 = \frac{\varrho_{(i,j)}\Delta\tau}{2Pr J^2_{(i,j)}\Delta\zeta} + \frac{\alpha_{(i,j)}\Delta\tau}{Pr J^2_{(i,j)}\Delta\zeta^2} - \frac{E\Delta\tau}{4\Delta\zeta\Delta\eta J_{(i,j)}} \quad (31\text{-a})$$

$$C_2 = -\frac{\varrho_{(i,j)}\Delta\tau}{2Pr J^2_{(i,j)}\Delta\zeta} + \frac{\alpha_{(i,j)}\Delta\tau}{Pr J^2_{(i,j)}\Delta\zeta^2} + \frac{E\Delta\tau}{4\Delta\zeta\Delta\eta J_{(i,j)}} \quad (31\text{-b})$$

$$C_3 = 1 - \frac{2\alpha_{(i,j)}\Delta\tau}{Pr J^2_{(i,j)}\Delta\zeta^2} - \frac{2\gamma_{(i,j)}\Delta\tau}{Pr J^2_{(i,j)}\Delta\eta^2} \quad (31\text{-c})$$

$$C_4 = \frac{\varpi_{(i,j)}\Delta\tau}{2Pr J^2_{(i,j)}\Delta\eta} + \frac{\gamma_{(i,j)}\Delta\tau}{Pr J^2_{(i,j)}\Delta\eta^2} + \frac{F\Delta\tau}{4\Delta\zeta\Delta\eta J_{(i,j)}} \quad (31\text{-d})$$

$$C_5 = -\frac{\varpi_{(i,j)}\Delta\tau}{2Pr J^2_{(i,j)}\Delta\eta} + \frac{\gamma_{(i,j)}\Delta\tau}{Pr J^2_{(i,j)}\Delta\eta^2} - \frac{F\Delta\tau}{4\Delta\zeta\Delta\eta J_{(i,j)}} \quad (31\text{-e})$$

$$C_6 = \frac{\beta_{(i,j)}\Delta\tau}{2Pr J^2_{(i,j)}\Delta\zeta\Delta\eta} \quad (31\text{-f})$$

$$C_7 = \left[\frac{\left(W_{(i,j)} + Q_{(i,j)} + N\hat{R}^2\theta_{(i,j)}\right)}{Pr}\right]\Delta\tau \quad (31\text{-g})$$

$$E = \Psi_{(i,j+1)} - \Psi_{(i,j-1)} \quad (31\text{-h})$$

$$F = \Psi_{(i+1,j)} - \Psi_{(i-1,j)} \quad (31\text{-i})$$

4- Stream Function Solving Method :-

$$\Psi^{n+1}_{(i,j)} = \Psi^n_{(i,j)} + \sigma\left(\Psi^{n+1}_{(i,j)} - \Psi^n_{(i,j)}\right) \quad (32)$$

5- Calculation of Average Axial Velocity :-

$$\overline{W} = \left(\sum_{i,j}^{Ni,Nj} W_{(i,j)}J_{(i,j)}\right)/J \quad (33)$$

6- Calculation of Bulk Temperature :-

$$\theta_b = \left(\sum_{i,j}^{Ni,Nj} \theta_{(i,j)}W_{(i,j)}J_{(i,j)}\right)/\overline{W}J \quad (34)$$

7- Calculation of Nusselt Number :-

$$Nu_b = \frac{\overline{W}_{(i,j)}(\hat{R}+1)}{4\theta_{b(i,j)}} \quad (35)$$

RESULTS AND DISCUSION:

Numerical investigations was conducted for different eccentricity ratios **ε** in different angular positions **φ₀** of the inner cylinder within the physical domain. The isotherms and streamlines for different **ε** and **φ₀** and the results for variation of eccentricity with Nusselt number were shown in figures [(2) to (8)], in which five angular positions of (φ_o=0°, 45°, 90°, 135°, 180°) and four eccentricities of (ε = 0, 0.25, 0.50, 0.75) where considered .

Isotherms & Streamlines:-

Figs. [(2) to (7)] illustrate the isotherms and streamlines for *Ra=200*, *Re=50*, *Pr=0.7*and $\hat{R}$*=2.6* with different values of **ε** and **φ₀**.

Pure conduction heat transfer is increased with eccentricity, which is revealed by the increasing in specific conductivity K_ε as a function of **ε**. Interpretation is as follows: because of

the narrowed gap in the large eccentricity annulus thermal convection by large recirculating vorticities become more and more difficult in contrast to the growing influence of the thermal conduction.

Fig. (2) shows the isotherms and streamlines for concentric annulus. The streamlines are symmetric with respect to the vertical line, there will be a stagnant region in the lower part of the gap, in this region the natural convection effect will be low and it is identical to the case of thermally steady state fluid flow between two horizontal plates, when the upper plate is much higher than the lower one.

Detailed isotherms and streamlines for eccentric annulus are presented in **Figs.[(2) to (7)]** respectively, the vortex strength current was un symmetric and the vortex strength will be increased in the wider part of the gap. Buoyancy plume will be deviated to the narrowed part of the gap and this deviation will be increased as ε increased due to the limitation in the fluid motion in the narrowed part and the buoyancy force will be unequal on each sides of the gap. As ε increased the buoyancy plume will be separated in the largest part of the gap due to the viscosity force.

In the narrowest part of the gap, the conduction dominancy is readily recognizable from the isotherm plots. Also, as seen from the streamline contours, more and more fluid is mobilized in the convection currents with decreasing φ_o to deliver thermal energy from the inner heated cylinder to the outer cold cylinder. It is noted that the positioned influence on the heat transfer is felt more strongly from the isotherm plots than from the streamlines, since the temperature inversion phenomenon becomes very distinguished as φ_o is decreased from (180° to 0°), this clearly indicates that the role of convection increases with lower φ_o. For high eccentricity the conduction dominating flow region at the narrowest gap of the annuli becomes locally stagnant which results in splitting of the core of the vortex in the constricted region into two sub vortices rotating in the same direction.

At first, the vortex core only is halvened, but as the gap is further narrowed local stagnant region grows large enough to bisect the whole vortex even much before the two cylinders come into contact. In the wider part of the eccentric annulus the vortex current is slowed down and location of its core is lowered as eccentricity increased. This clearly indicates that the relative role of convection is steadily decreased with higher eccentricity, whereas the overall heat transfer is changed to increasing pattern after a slight decrease near $\varepsilon=0.50$. This is again surely due to the contribution of conduction for increased eccentricities. It is noted that the decreased degree of plume development and temperature inversion with higher eccentricities and the slowed –down stream speed together with the vortex halvening and all consistently related with the magical interaction between the conduction and the convection discussed so far.

Also, the radiation effect plays a significant role with the position of the inner cylinder. Once the medium participates in the absorption and emission of radiation, the medium temperature tends to move uniform. Further more, as the participating medium alternates the radiation more, a direct interaction of the inner hotter cylinder with the cold outer cylinder, i.e., surface radiation, is decreased.

This is clearly evidenced by observing a downward shift of the isotherm closer to the outer cold cylinder for both cases of concentric and eccentric annulus as ***N*** increased. When the inner cylinder is displaced downward as shown in **Fig. (3)**, the location of the convective cell center barely changes. Moreover compared to the pervious case, ***N*** has an insignificant effect in the medium temperature variation; this is derived from the fact that the thermo-fluid dynamics characteristics become buoyancy dominant. In other wards, when the inner cylinder is located at the downward positions the internal buoyancy-induced flow becomes stronger, which in turn results in higher heat transfer rate.

The angular positions of $\varphi_o=0^o$ and $\varphi_o=180^o$ are two special cases in the eccentric annulus, for these two special cases, there is no global circulation. As a consequence, the flow and thermal fields are symmetric with respect to the vertical line connecting the centers of two cylinders. This can be clearly shown if **Figs.[(3) and (7)].** When the inner cylinder is moved near the bottom, the outer cylinder has a boundary layer every where, when the inner cylinder is moved near the top, there is no boundary layer on the bottom portion of the outer cylinder.

For $\varphi_o=0^o$ it is evident that the convective flows are both larger and stronger than the concentric annulus for low eccentricity ratio (ε=0.25, ε=0.5) but for large eccentricity for example (ε=0.75), the only effect which can be recognized is that the reduction in the rate of heat transfer and this is again due to the stagnant region in the narrowest gap.

Also, $\varphi_o=180^o$ provides least favored circumstance for the development of the heat transfer, both the size and strength of the fluid flow are markedly reduced.

On the other hand, it was found that the global circulation of the flow does exist around the hot inner cylinder for eccentricity cases of ($\varphi_o=45^o$, 90° and $\varphi_o=135^o$) as shown in **Figs. [(4), (5) and (6)]** . For these cases, the computed Ψ_{max} has a relatively large value. The magnitude of the circulation varies form zero for a concentric annulus to a maximum value for an intermediate eccentricity and back to zero for $\varepsilon\approx 1$. This is because for $\varepsilon = 0$ the flow field is symmetric, and no global circulation exists. When ε tends toward **1**, the two cylinder surfaces are very close at some point so that there is no sufficient space for fluid flow. Therefore, the global circulation for this case is very weak.

As can be shown from **Fig. (6)** that for $\varphi_o=135^o$ and ε = 0.50 and ε = 0.75, there will be a small vortex in the upper part of the gap. This small vortex will cause a deviation to the buoyancy plume to the largest part of the gap.

Effect of Eccentricity on Nu:

Fig.(8) illustrates the variation of ***Nu*** with angular location φ_o for different ε. For fixed eccentricity ε for example (ε=0.25), and the inner cylinder is moved circumferentially, by increasing φ_o , ***Nu*** will be decreased. This clearly indicates that the role of convection increases with lower φ_o .

For fixed angular position for example ($\varphi_o=90^o$) and different eccentricity, ***Nu*** will be decreased as ε increased from (0.25 to 0.75). That the relative role of convection is steadily decreased with higher eccentricity, this is again surely due to the contribution of conduction for increased eccentricity.

A correlation equation for the plotted curve of Nu for any eccentricity ratio and angular position had been written to show the eccentricity effect on the rate of heat transfer. Curve fitting method (Least square method) with two programs (Statistica and DGA) which were used to form this equation.

$$Nu = a_1 + b_1 . \varepsilon^{c_1} . \cos\varphi_o \qquad (36)$$

The above equation is valid for Re=50, Pr=0.7, Ra=200, $\hat{R}$=2.6 and $\varphi_o = 0°, 45°, 90°, 135°, 180°$. Where, a_1, b_1 and c_1 are constants and there values are as follows:-

Parameter	Estimate
a_1	6.80 for $\varepsilon = 0.25$
	6.03 for $\varepsilon = 0.50$
	5.94 for $\varepsilon = 0.75$
b_1	0.5
c_1	-0.64

Comparison of Results:

A comparison was made with the isotherms and streamlines resulted from the work of [**Ho, Lin and Chen 1989**] for natural convection heat transfer in an eccentric horizontal annulus with ($Ra=10^6$, ε=0.625 and $\varphi_o=180^o$) as shown in **Fig.(9),** the results show a good agreement .

CONCLUSIONS:

For fixed eccentricity ratio and radius ratio, the overall heat transfer increased due to the expanded convection as the angular position φ_o of the inner cylinder decreased. And for a fixed angular position, when the inner cylinder was moved outward from the concentric position along a horizontal line, convection heat transfer decreases contrary to the conduction heat transfer which grows with a faster rate. It was found that at ε=0.25 and $\varphi_o=0^o$, maximum heat transfer will be recognized.

REFERENCES:

Akeel A. M. Al−Sudani, 2005, "An Investigation Into Laminar Combined Convection Heat Transfer Through Concentric Annuli"، PhD. Thesis, University of Technology, Mechanical Engineering Department .

Ho C. J., Lin Y. H. and Chen T. C., 1989, "A Numerical Study of Natural Convection in Concentric and Eccentric Horizontal Cylindrical Annuli with Mixed Boundary Conditions", Int. J. Heat and Fluid Flow, Vol. 10, No. 1, PP. 40-47.

Kaviany M., 1986, " Laminar Combined Convection in a Horizontal Annulus Subjected to Constant Heat Flux Inner Wall and Adiabatic Outer Wall", J. Heat Transfer, ASME, Vol.108, PP.392-397.

Kotake S. and Hattori N., 1985, "Combined Forced and Free Convection Heat Transfer for Fully – Developed Laminar Flow in Horizontal Annuli", J. Heat and Mass Transfer, Vol.28, No.11, PP.2113-2120.

Shu C. and Wu Y. L., 2001, "Domain Free Discretization Method for Doubly Connected Domain and Its Applications to Simulate Natural Convection in Eccentric Annuli", Internet, Science Direct, Vol. 191, Issues 17-18, PP. 1827-1841 .

William T. Snyddi, 1963, "An Analysis of Slug Flow Heat Transfer in an Eccentric Annulus", A.I.Ch.E. Journal, Vol. 9, No. 4, PP. 503-506 .

Yasin K. Salman, Jalal M. Jalil and Ahmed F. Khudheyer, 2006, "Experimental Study of Mixed Convection Heat Transfer to Thermally Developing Air Flow in a Horizontal Rectangular Duct", convection heat transfer through concentric annuli"، University of Baghdad .

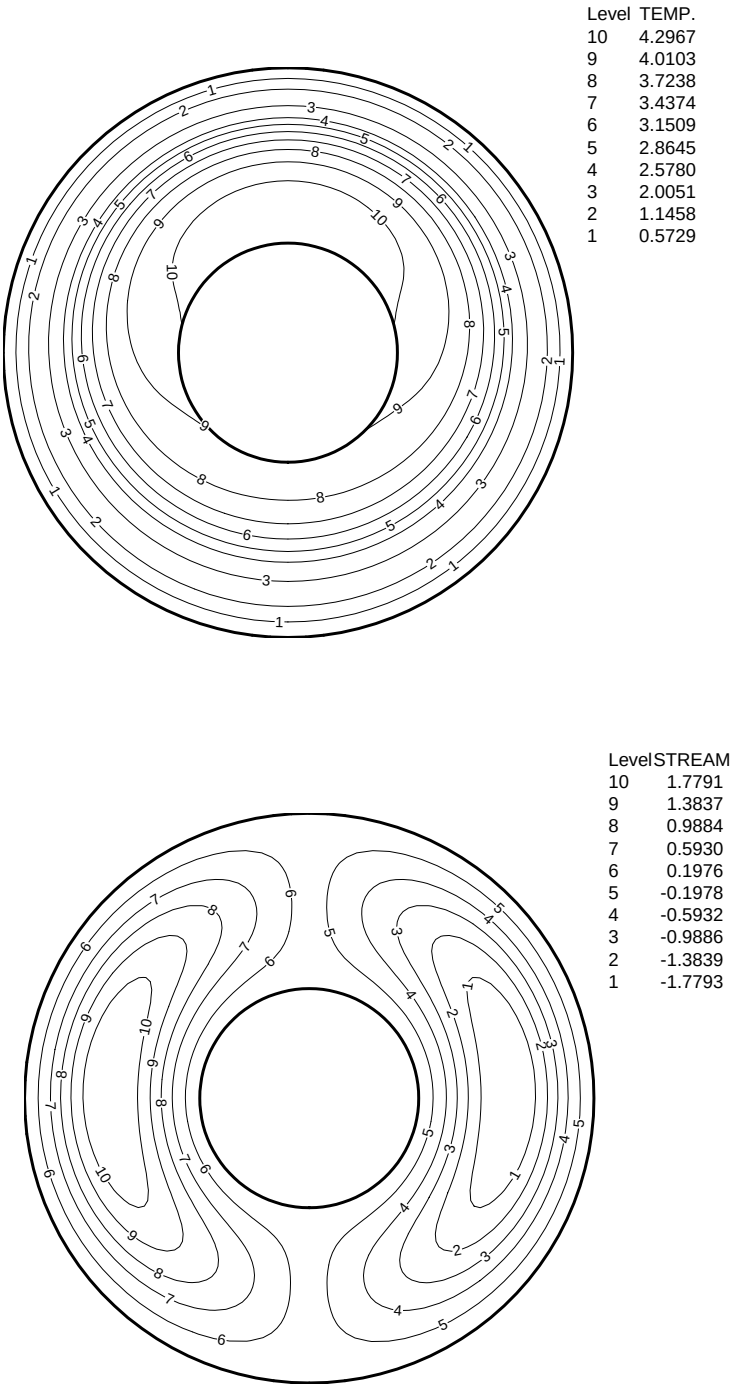

Figure (2)
Isotherms & Streamlines for Concentric Annulus ($\varphi_o=0^o,\varepsilon=0.0$)
Ra=200, Re=50, Pr=0.7, $\hat{R}$=2.6, N=3, $\hat{t}$=1

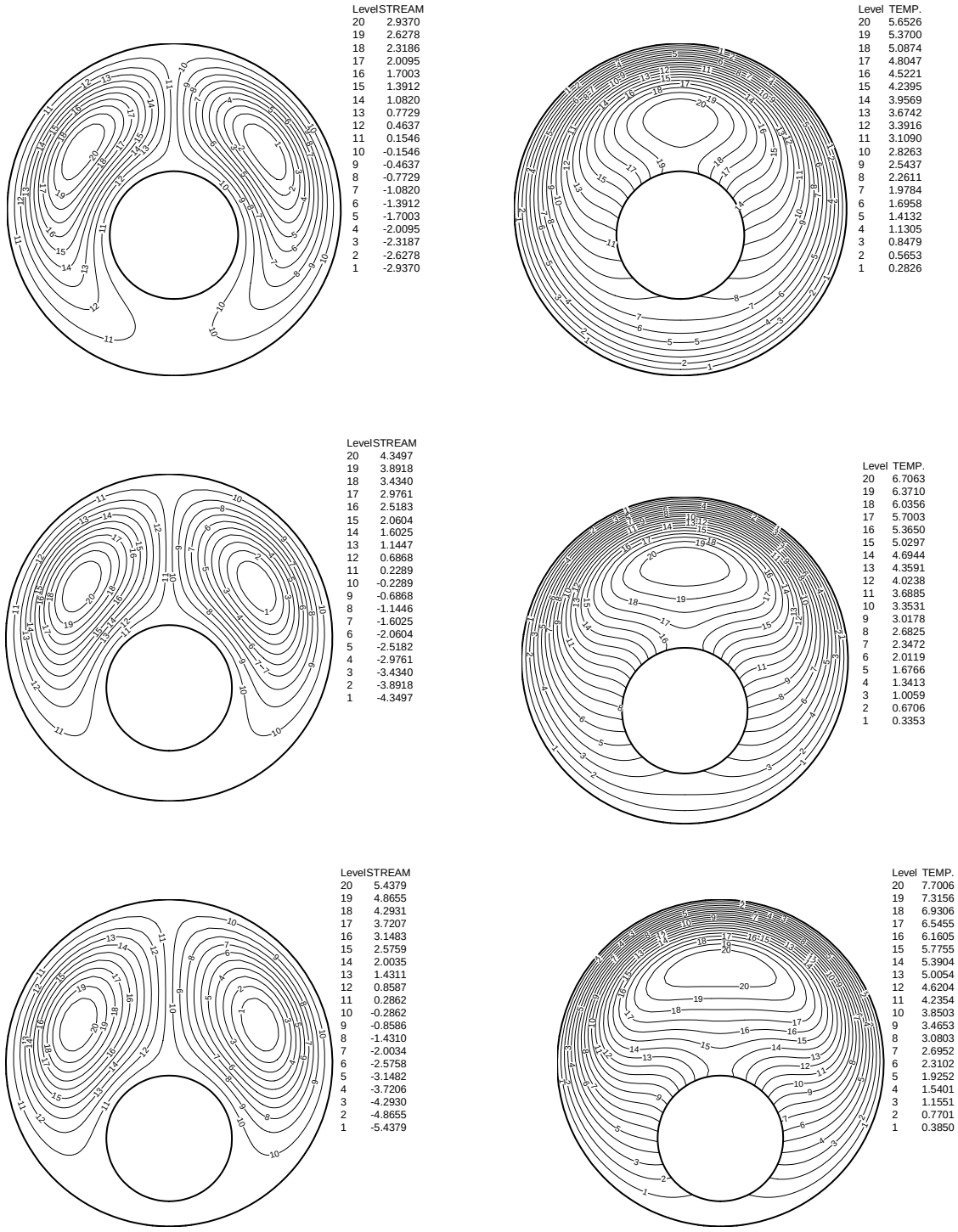

Figure (3)
Isotherms & Streamlines for Eccentric Annulus ($\varphi_o=0^o$)
Ra=200, Re=50, Pr=0.7, $\hat{R}$=2.6, N=3, $\hat{t}$=1

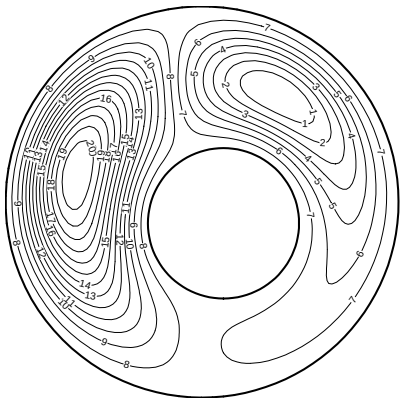

Level	STREAM
20	3.7173
19	3.4189
18	3.1206
17	2.8222
16	2.5239
15	2.2255
14	1.9271
13	1.6288
12	1.3304
11	1.0320
10	0.7337
9	0.4353
8	0.1370
7	-0.1614
6	-0.4598
5	-0.7581
4	-1.0565
3	-1.3549
2	-1.6532
1	-1.9516

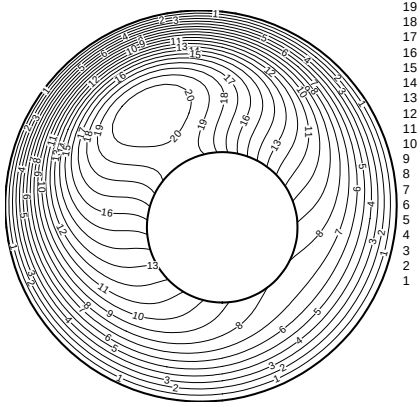

Level	TEMP.
20	5.7227
19	5.4365
18	5.1504
17	4.8643
16	4.5781
15	4.2920
14	4.0059
13	3.7197
12	3.4336
11	3.1475
10	2.8613
9	2.5752
8	2.2891
7	2.0029
6	1.7168
5	1.4307
4	1.1445
3	0.8584
2	0.5723
1	0.2861

Level	STREAM
20	4.8169
19	4.3771
18	3.9373
17	3.4975
16	3.0578
15	2.6180
14	2.1782
13	1.7385
12	1.2987
11	0.8589
10	0.4191
9	-0.0206
8	-0.4604
7	-0.9002
6	-1.3400
5	-1.7797
4	-2.2195
3	-2.6593
2	-3.0990
1	-3.5388

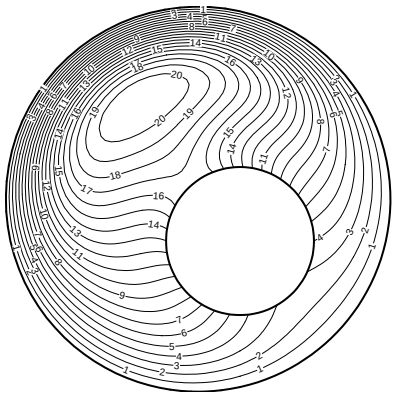

Level	TEMP.
20	6.8492
19	6.5067
18	6.1643
17	5.8218
16	5.4793
15	5.1369
14	4.7944
13	4.4520
12	4.1095
11	3.7670
10	3.4246
9	3.0821
8	2.7397
7	2.3972
6	2.0548
5	1.7123
4	1.3698
3	1.0274
2	0.6849
1	0.3425

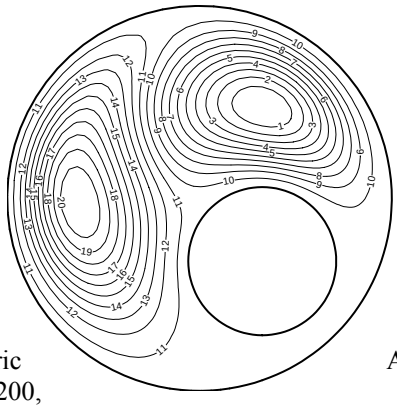

Level	STREAM
20	5.2179
19	4.6606
18	4.1033
17	3.5460
16	2.9886
15	2.4313
14	1.8740
13	1.3167
12	0.7594
11	0.2020
10	-0.3553
9	-0.9126
8	-1.4699
7	-2.0273
6	-2.5846
5	-3.1419
4	-3.6992
3	-4.2565
2	-4.8139
1	-5.3712

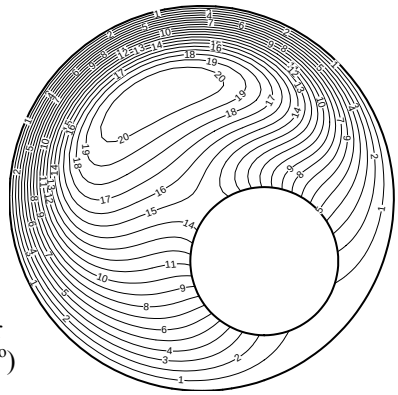

Level	TEMP.
20	7.8742
19	7.4805
18	7.0868
17	6.6930
16	6.2993
15	5.9056
14	5.5119
13	5.1182
12	4.7245
11	4.3308
10	3.9371
9	3.5434
8	3.1497
7	2.7560
6	2.3623
5	1.9685
4	1.5748
3	1.1811
2	0.7874
1	0.3937

Figure (4) Isotherms & Streamlines for Eccentric Annulus (φ_o=45°) Ra=200, Re=50, Pr=0.7, $\bar{R}$=2.6, N=3, $\bar{t}$=1

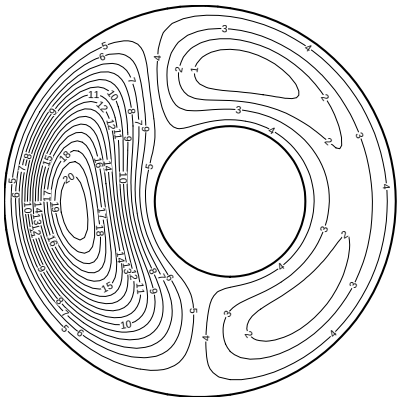

Level	STREAM
20	4.2525
19	3.9824
18	3.7124
17	3.4423
16	3.1723
15	2.9022
14	2.6322
13	2.3621
12	2.0920
11	1.8220
10	1.5519
9	1.2819
8	1.0118
7	0.7418
6	0.4717
5	0.2017
4	-0.0684
3	-0.3385
2	-0.6085
1	-0.8786

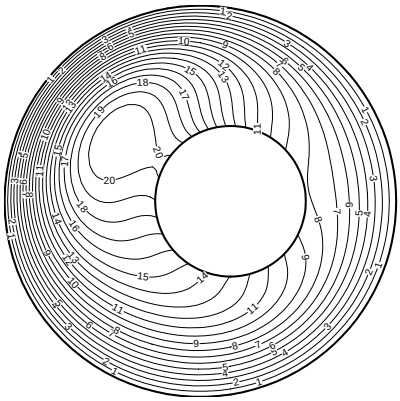

Level	TEMP.
20	5.8767
19	5.5829
18	5.2891
17	4.9952
16	4.7014
15	4.4076
14	4.1137
13	3.8199
12	3.5260
11	3.2322
10	2.9384
9	2.6445
8	2.3507
7	2.0569
6	1.7630
5	1.4692
4	1.1753
3	0.8815
2	0.5877
1	0.2938

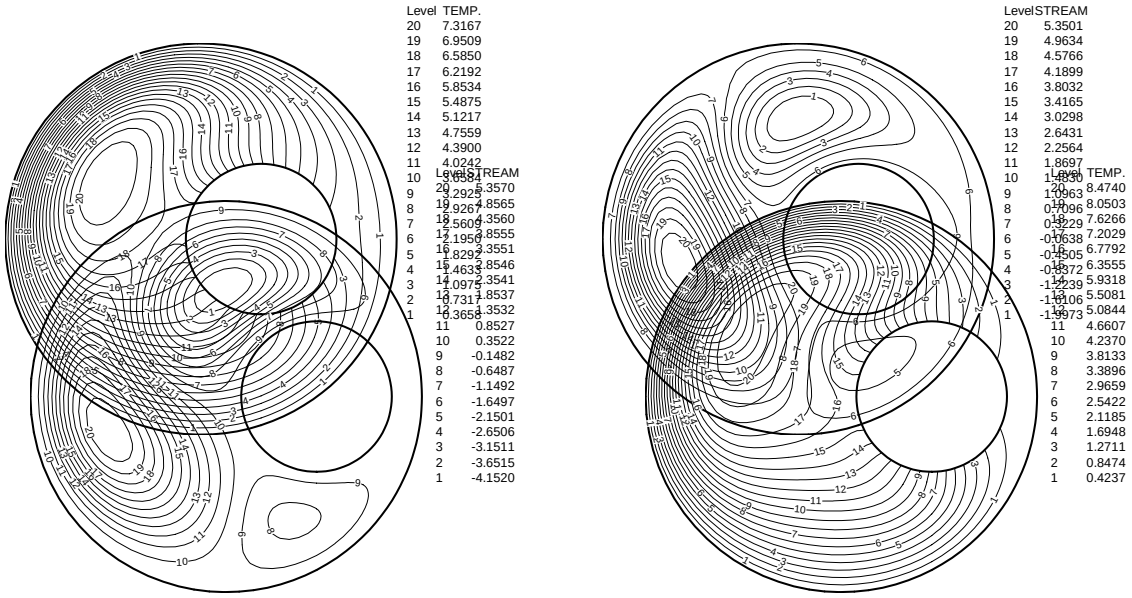

Figure (5)
Isotherms & Streamlines for Eccentric Annulus (φ_o=90°)
Ra=200, Re=50, Pr=0.7, $\hat{R}$=2.6, N=3, $\hat{t}$=1

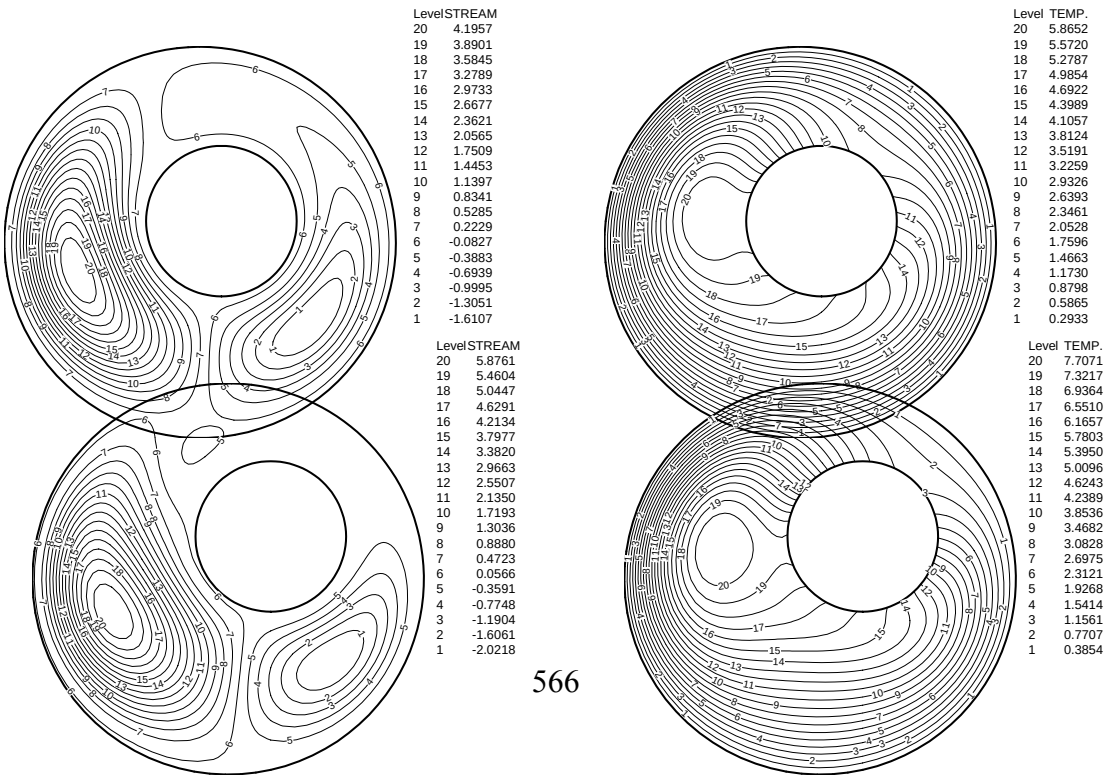

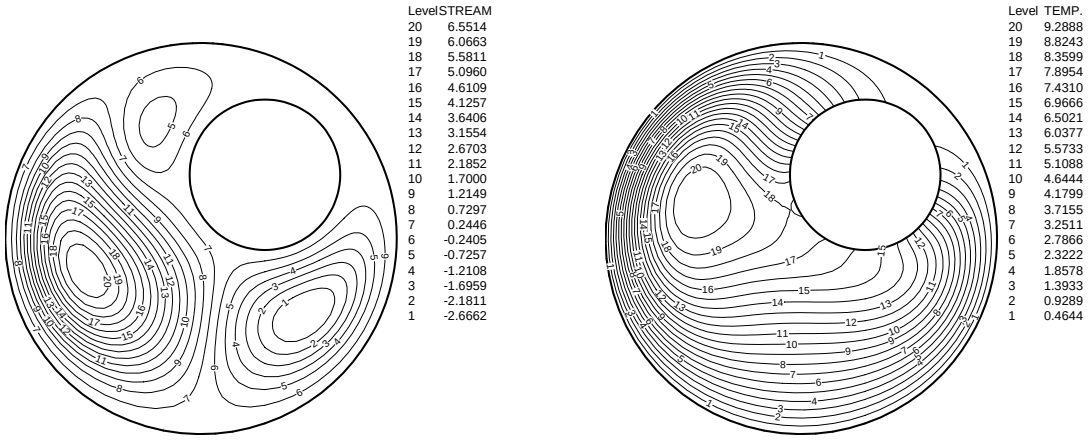

Figure (6)
Isotherms & Streamlines for Eccentric Annulus (φ_o=135°)
Ra=200, Re=50, Pr=0.7, $\bar{R}$=2.6, N=3, $\bar{t}$=1

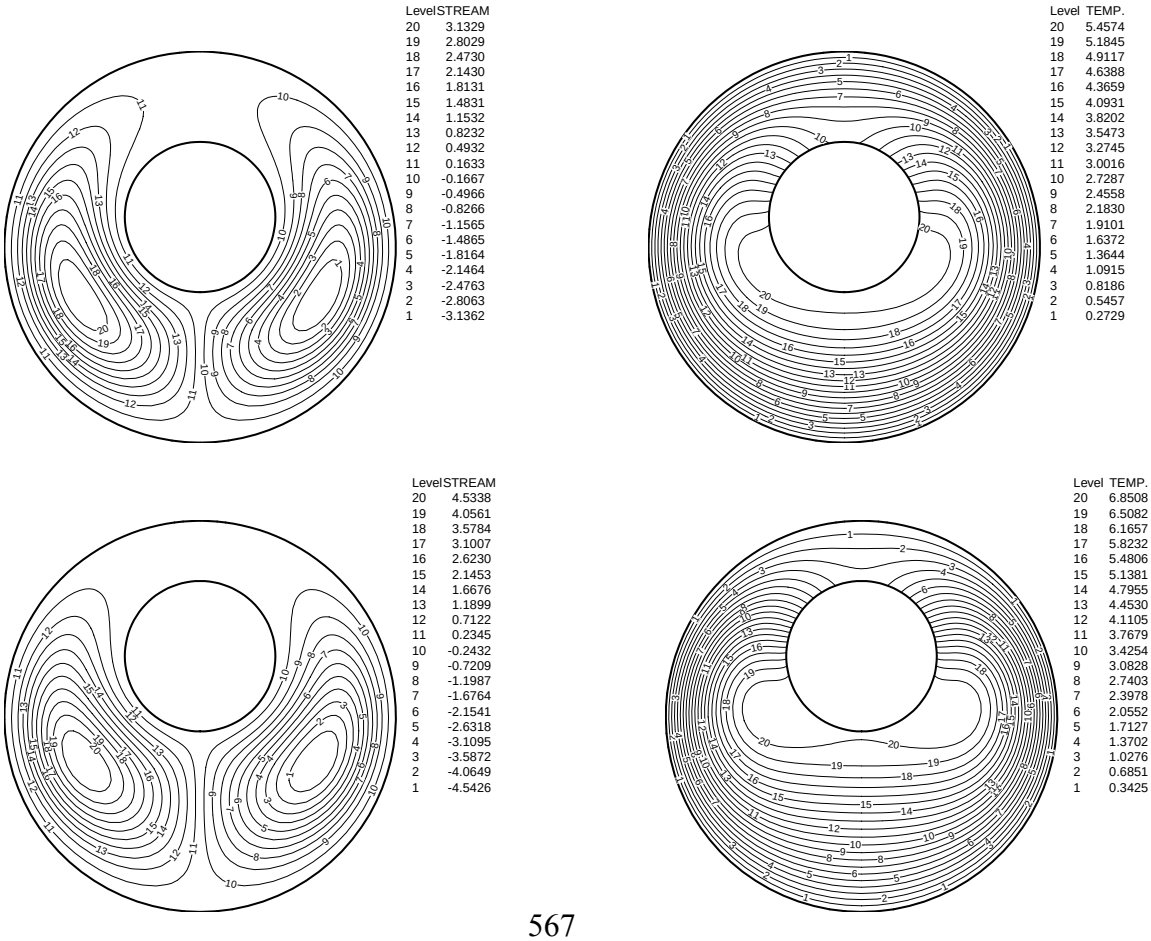

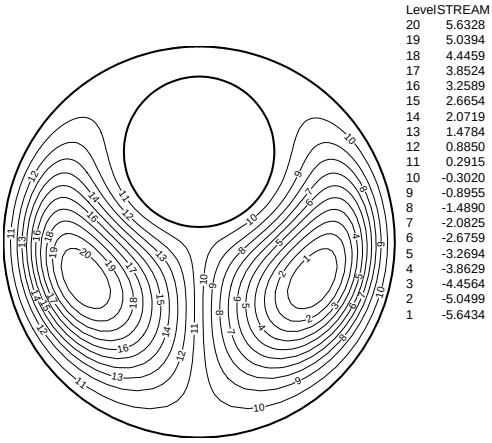

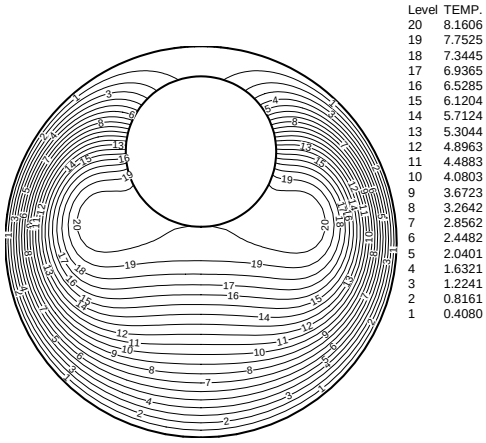

Figure (7)
Isotherms & Streamlines for Eccentric Annulus (φ_o=180°)
Ra=200, Re=50, Pr=0.7, $\bar{R}$=2.6, N=3, $\hat{t}$=1

Figure (8) Effect of ***Nu*** Eccentricity on Present Work

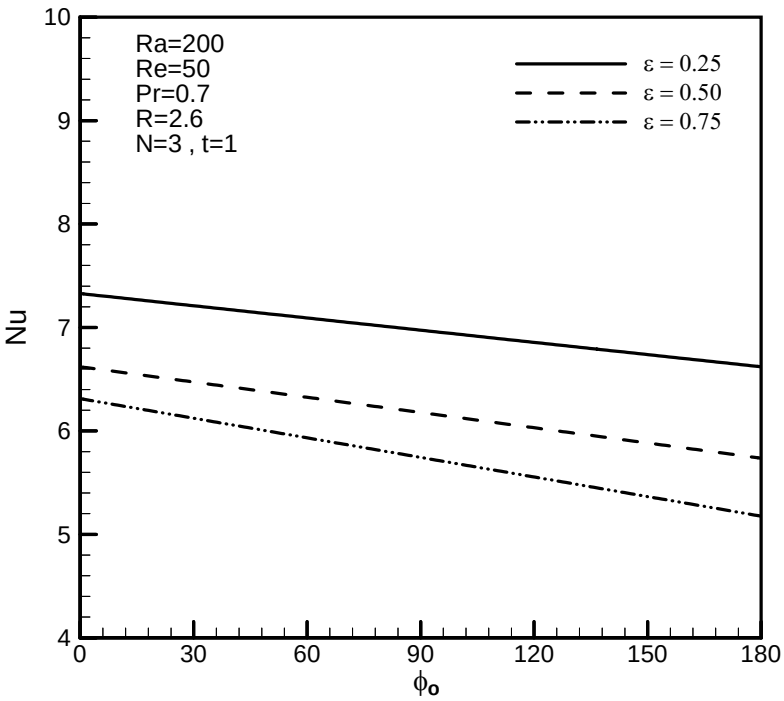

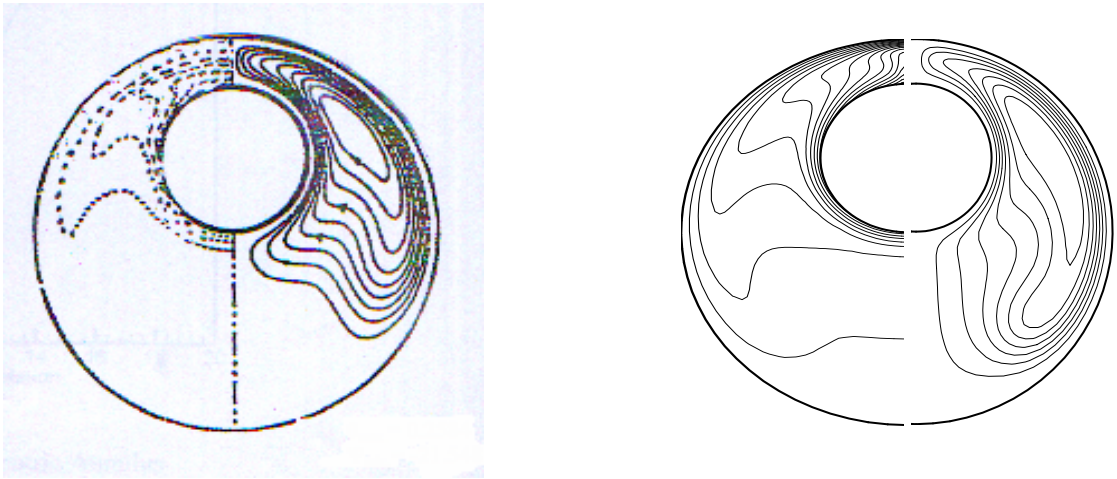

$\theta_{max.}$= 0.2942
$\Psi_{min.}$= -25.0405

$\theta_{max.}$= 0.2584
$\Psi_{min.}$= -21.548

Figure (9)
Comparison of Isotherms & Streamlines for Eccentric Annulus
(φ_o=180°,ε=0.625), Ra=10^6, Pr=0.7, $\hat{R}$=2.6, N=0, $\hat{t}$=0

NOMENCLATURE:
LATIN SYMBOLS:

Symbol	Description	Unit
$\hat{R}$	Radius Ratio ($\hat{R} = \frac{r_o}{r_i}$)	---
$\hat{t}$	Optical Thickness ($\hat{t} = k_r \mathrm{De}$)	---
A	Axial Pressure Gradient ($\mathrm{A} = -\frac{4\rho\nu^2 Re}{\mathrm{De}^3}$)	N/m^3
C	Axial Temperature Gradient ($\mathrm{C} = \frac{\partial T}{\partial z}$)	K/m
De	Hydraulic Diameter De = 2(r_o - r_i)	m
e	Space Between the Centers of the Inner and Outer Cylinders	m
g	Gravitational Acceleration	m/s^2
J	Jacobean of Direct Transformation	---
K	Thermal Conductivity of the Air	W/m.K
K_r	Volumetric Absorbtion Coefficient	m^{-1}
N	Radiation-Conduction Parameter ($N = \frac{4\sigma\epsilon T_W^3}{k k_r}$)	---
n	Dimensionless Outer Normal Direction	---
Ni	Number of Gridlines in the φ-direction	---
Nj	Number of Gridlines in the r-direction	---

Nu_b	Bulk Nusselt Number	---
P	Normalized Air Pressure	---
p	Air Pressure	N/m^2
Pr	Prandtl No. ($Pr = \frac{\nu}{\alpha}$)	---
Ra	Rayleigh Nnmber ($Ra = \frac{g\beta C De^4}{\nu\alpha}$)	---
Symbol	Description	Unit
Re	Reynolds Number ($Re = \frac{ADe^2}{4\rho\nu^2}$)	---
R_i	Dimensionless Inner Cylinder Radius	---
r_i	Inner Cylinder Radius	m
R_O	Dimensionless Outer Cylinder Radius	---
r_o	Outer Cylinder Radius	m
T	Air Temperature	K
t	Time	Second
u, v, w	Velocity Components in x, y and z Direction Respectively	m/s
U, V, W	Dimentionless Velocity Components in X, Y and Z Direction Respectively	---
x, y, z	The physical Coordinates of The Annulus	m
X, Y, Z	The Dimensionless Physical Coordinates of The Annulus	---

GREAK SYMBOLS:

Symbol	Description	Unit
φ	Angular coordinate around inner cylinder	Degree
ϱ, ϖ, γ	Coefficient of Transformation of BFC.	---
φ_o	Angular position for the inner cylinder	Degree
α	Thermal Diffusivity	m^2/s
	Coefficient of Transformation of BFC	---
β	Coefficient of Thermal Expansion	1/K
	Coefficient of Transformation of BFC	---
ε	Dimensionless Eccentricity ($\varepsilon = e / De$)	---
ζ , η	Coordinates in The Transformed Domain	m
θ	Dimensionless Air Temperature ($\theta = \frac{(T_w - T)}{PrCDe}$)	---
σ	Stefan Boltizman Constant	W/m^2K^4
	Relaxation Parameter	---
τ	Dimensionless Time ($\tau = \frac{\nu t}{De^2}$)	---
υ	Kinematic Air Viscosity	m^2/s
Ψ	Dimensionless Air Stream Function	---
Ω	Dimensionless Air Vorticity	---
ϵ	Emissivity	---